Supporting Information

Kawasaki et al. 10.1073/pnas.1318761111

SI Materials and Methods

Cells. NIH 3T3 mouse embryo fibroblasts (American Tissue Culture Collection, CRL-1658) were cultured in DMEM with 10% (vol/vol) FBS (Invitrogen). Primary mouse embryo fibroblasts (MEFs) from the various wild-type mouse strains were generated from 13.5 d postcoitum embryos as previously described (1) and cultured in DMEM supplemented with 10% (vol/vol) FBS, glutamine (200 mM), penicillin (100 units/mL), and streptomycin (100 mg/mL). Forty-eight hours before experiments, MEFs were starved in DMEM with 0.5% FBS for 24 h followed by 2 h in DMEM without FBS. MEFs were used within two passages of collection. CarB skin carcinoma cells (2) were provided by Allan Balmain (University of California, San Francisco, UCSF). These cells express high levels of VEGF and SDF1. CarB cells were cultured in DMEM with 10% (vol/vol) FBS and 0.1 mM of nonessential amino acids.

Mice. All animal experiments were in full compliance with the UCSF Institutional Animal Care and Use Committee, which is Association for Assessment and Accreditation of Laboratory Animal Care accredited. A total of 5×10^5 syngeneic CarB cells were injected s.c. and bilaterally into the dorsolateral aspect of mice to induce an angiogenesis stimulus. Blood was drawn by terminal cardiac puncture at time points from day 0 to day 7 post-CarB inoculation. TMI-005 (50 mg/kg), LY2109761 (100 mg/kg), or vehicle was delivered by oral gavage in a polytroned suspension in 1% (wt/vol) sodium carboxymethylcellulose (Hercules), 0.5% sodium lauryl sulphate (Sigma), 0.085% polyvinylpyrrolidone K30 (ISP Tecnologies, Inc.), 0.05% Dow Corning antifoam. Drug or vehicle was administered two times per day every day from 1 d before CarB inoculation. A total of 20 μL of blood was used for HEMAVET analysis. A total of 100 μL of blood was used for FACS analysis, by incubating with the antibodies, FITC-CD13 (BD Biosciences), PE-VEGFR2 (BD Biosciences), PerCP-CD45 (BD Biosciences), and APC-CD117 (BD Biosciences) in 100 μL of FACS buffer (0.5% BSA in PBS) for 30 min. For the isotype control, FITC–anti-rat $IgG1_k$, PE–anti-rat IgG2a, PerCP–anti-rat IgG2b, and APC–anti-rat IgG2b were used. Erythrocytes were hemolyzed twice using 200 μL of ACK lysing buffer (Lonza). The remaining blood cells were suspended in 300 μL of FACS buffer and analyzed by FACS Calibur (BD). $CD45^-$ cells were gated to exclude leukocytes and then classified according to CD13 and CD117 status. CEPCs were classified as $CD45^-$ $CD13^+$ $CD117^+$ (3, 4). More than 90% of cells that were $CD13^+$ were also $VEGFR2^+$ and vice versa; therefore, this latter marker was not used in all analyses. The cell numbers were normalized for absolute cell number per microliter, based on HEMAVET analysis (cells per microliter).

Immunocytochemistry. Immunocytochemistry (ICC) was carried out on 4% (wt/vol) PFA-fixed MEF cells. Cells were blocked for 1 h in 5% (vol/vol) FBS (Invitrogen), 0.3% Triton. Primary rabbit anti-total Smad2 (D43B4) XP antibody (Cell Signaling) was added at a 1:100 dilution in blocking solution, incubated overnight at 4 °C, washed in PBS followed by 1 h of incubation at room temperature with secondary antibody Alexa 488 (1:100) in blocking solution. Cells were then washed three times in PBS and mounted with DAPI (ProLong Gold antifade, Invitrogen). Images were captured at 40× magnification using a LSM 510 META (Zeiss) confocal microscope. NIH ImageJ was used to determine intensity of nuclear staining. A region of interest (ROI) was drawn around each nucleus to be measured and average fluorescence intensity of a pixel in the ROI was measured for each time point, and divided by its surface area. Quantification used six fields of view per cell line ($n = 25$–30 cells).

CAGA-Luciferase Assay. Twenty-four hours after plating, NIH 3T3 cells were transfected with pGL2-CAGAluc and pRL-renilla and cotransfected with pcDNA3, pcDNA3.NIH-ADAM17, pcDNA3-$Adam17^{Asp113}$, pcDNA3-$Adam17^{Val613}$, or pcDNA3.C57-ADAM17, using Lipofectamine 2000 (Invitrogen). Twenty-four hours following transfection, the cells were lysed and the lysate was subjected to the Dual-Luciferase Reporter Assay system (Promega). Luminescence from Firefly and Renilla luciferases were measured by GloMax 96 Microplate Luminometer (Promega), and data presented as the ratio of Firefly to Renilla luciferase.

Human subjects. Dutch Caucasians and Dutch Antillean Blacks were selected from a panel consisting of probands and family members screened for hereditary hemorrhagic telangiectasia (HHT). All manifestations of HHT were recorded for both probands and family members. The clinical diagnosis of HHT was established according to the Curaçao criteria (5), which are clinical features of epistaxis, multiple telangiectases, visceral arteriovenous malformation (AVM), and a first-degree relative with HHT. A diagnosis of HHT is considered definitive if three criteria are present, possible if two criteria are present, and unlikely if fewer than two criteria are present. Mutation carrier status was confirmed by molecular analysis. Most probands and family members were screened for visceral manifestations at St. Antonius Hospital, which specializes in the diagnosis and treatment of HHT. In most cases, screening for the presence of a pulmonary AVM (PAVM) was performed routinely by chest radiography and by measuring partial oxygen tension in arterial blood and, if abnormal, followed by the 100% oxygen right-to-left shunt test. Patients with a suspected PAVM were offered conventional angiography, digital subtraction angiography of the pulmonary arteries, or computed tomography (CT) of the chest. In some patients, PAVMs were diagnosed using high-resolution CT and/or contrast transthoracic echocardiography.

French HHT clinical diagnosis was also established according to the Curaçao criteria (5). Mutation carrier status was confirmed by molecular diagnosis (heteroduplex analysis or denaturing high performance liquid chromatography and sequencing). Screening for PAVMs was recommended to asymptomatic patients and accepted by a majority of them. The diagnosis of pulmonary involvement was made either in patients presenting symptoms (for example, dyspnea and cyanosis) or complications (mainly brain abscess) or in asymptomatic patients with HHT who underwent screening using contrast transthoracic echocardiography, chest radiograph, and/or oxygen shunt test as described. The 222 French patients included in the present study all carried a mutation in either *ENG* or *ACVRL1*, and 43% of them had a PAVM (74% for patients with HHT1 and 27% for patients with HHT2). Familial structures included 111 singletons, 40 duos, two trios, five quartets, and one family with five individuals. Study protocols were approved by local ethics committees at all institutions, and informed consent was obtained from each subject before participation in the studies. All research involving human samples was approved by the Institutional Review Boards of each institute: The UCSF Committee on Human Research and the respective Medical Ethics Committees of St. Antonius Hospital, Nieuwegein, The Netherlands, and Lyon University Hospital, France.

Human SNP selection. Independent (linkage disequilibrium $r2 < 0.7$) tag-SNPs within *ADAM17* ($n = 6$) and gene centric SNPs within the syntenic region of *TGFBM3b* on 2p25 ($n = 175$) were selected on the basis of being nonsynonymous coding polymorphisms, potential splice site variants, or inferred to disrupt important gene regulatory sites (that is, microRNAs and tran-

scription factor binding sites, and so on) using the UCSC genome server. We further looked for SNPs located in highly conserved regions in the 3′ UTR. Selected SNPs were estimated to give ~85% coverage of any chosen gene.

Human genotyping and quality control. Initial genotyping of the Dutch cohort was performed using 750-ng–labeled genomic DNA hybridized to a custom Illumina chip. Genotyping for the extension and replication studies, and for fine mapping, was performed using Sequenom MALDI-TOF mass spectrometry. No significant difference in call rates between cases and controls was seen. Markers that deviated significantly from Hardy–Weinberg equilibrium were excluded ($P < 0.05$, Hardy–Weinberg) or if they had a call rate of <95% in the entire cohort.

Human Genetics Analysis. Familial association analysis was carried out using the gamete competition (GC) model implemented in the software package MENDEL (6). The GC model is an application of the Bradley–Terry method of ranking that compares the observed to the expected (50%) number of transmissions of the at-risk allele from heterozygous parent to affected offspring, and we used genotype data from both affected and unaffected family members because the model uses full pedigree data.

1. Xu J (2001) Preparation, culture, and immortalization of mouse embryonic fibroblasts. *Current Protocols in Molecular Biology* (Wiley, New York).
2. Stoler AB, Stenback F, Balmain A (1993) The conversion of mouse skin squamous cell carcinomas to spindle cell carcinomas is a recessive event. *J Cell Biol* 122(5): 1103–1117.
3. Mund JA, Estes ML, Yoder MC, Ingram DA, Jr., Case J (2012) Flow cytometric identification and functional characterization of immature and mature circulating endothelial cells. *Arterioscler Thromb Vasc Biol* 32(4):1045–1053.
4. Shaked Y, et al. (2005) Genetic heterogeneity of the vasculogenic phenotype parallels angiogenesis: Implications for cellular surrogate marker analysis of antiangiogenesis. *Cancer Cell* 7(1):101–111.
5. Faughnan ME, et al.; HHT Foundation International - Guidelines Working Group (2011) International guidelines for the diagnosis and management of hereditary haemorrhagic telangiectasia. *J Med Genet* 48(2):73–87.
6. Lange K, Sinsheimer JS, Sobel E (2005) Association testing with Mendel. *Genet Epidemiol* 29(1):36–50.

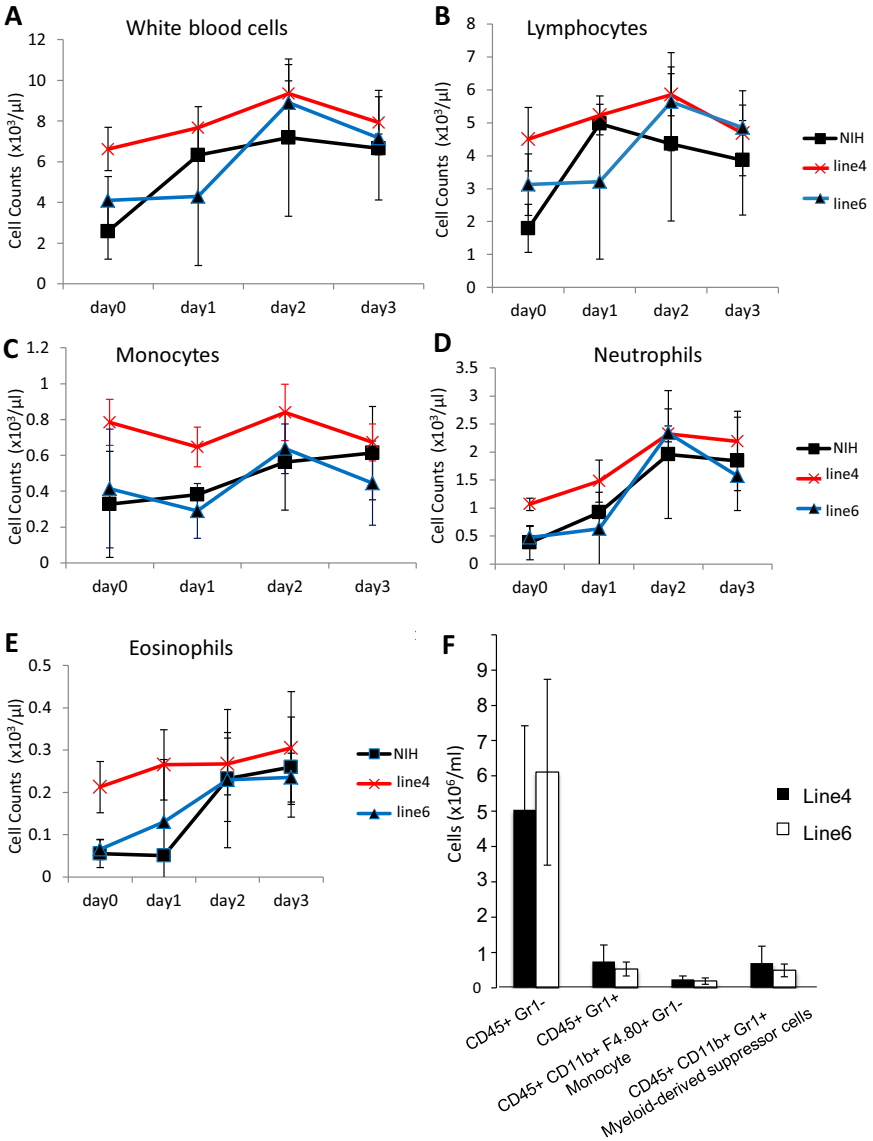

Fig. S1. No change in normal blood cell types 24 h after the angiogenic stimulus. (*A–E*) Blood was harvested at the indicated time points after the angiogenic stimulus and analyzed by Hemavet analysis. (*F*) Blood was harvested 24 h after the angiogenic stimulus and analyzed by FACS for the indicated markers. Each data point represents four mice of each genotype, and each experiment was independently reproduced three times.

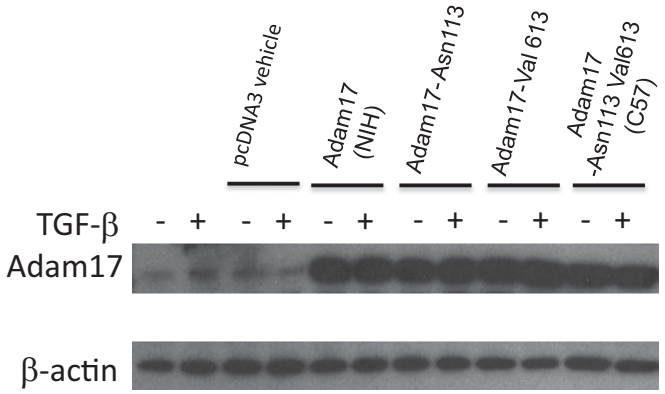

Fig. S2. Equivalent protein expression level of ectopic ADAM17 variants in NIH 3T3 cells. Cells were cotransfected with pGL2-CAGAluc and pRL-renilla (*Left*), together with pcDNA3, pcDNA3.NIH-ADAM17, pcDNA3-*Adam17*^{Asp113}, pcDNA3-*Adam17*^{Val613}, or pcDNA3.C57-ADAM17 (as indicated), using Lipofectamine 2000 (Invitrogen). Cells were incubated with or without TGFβ and 24 h later, cell lysates were assayed for luciferase reporter activity (Fig. 4) and proteins subjected to Western analysis using the indicated antibodies.

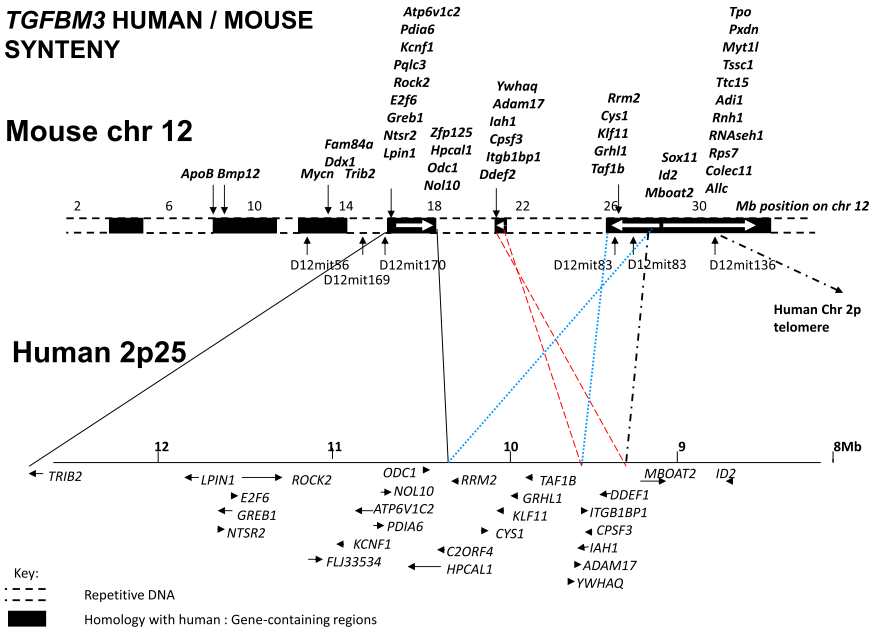

Fig. S3. Cartoon map comparing organization of *TGFBM3* in human compared with mouse. Mouse genome (*Upper*) and human genome (*Lower*) drawn roughly to scale and aligned to indicate genomic rearrangements that have occurred during evolution, including genomic inversions and insertions of repetitive DNA. Hence at *TGFBM3,* the mouse genome is considerably rearranged compared with human and has extensive expanses (megabases) of repetitive DNA, which are gene deserts (in white) between gene-rich islands (in black). White arrows within the black blocks of the mouse genome indicate directionality of gene order with respect to the human genome. Small arrows and arrowheads indicate genes in human and their orientation on the genome.

Table S1. Genome scan of NIH, C57, 129, line 4, and line 6 congenic mice

Table S1

gDNA from two representative mice of each strain were SNP genotyped using a custom array designed and run using the Illumina GoldenGate genotyping platform by the UCSF Genome Core Facility. Additional simple sequence repeat and SNP markers (Sequenom) were genotyped at critical regions of chromosome 12 for fine mapping of recombination endpoints and results integrated with this dataset. Deviations from an NIH genotype are highighted according to a color code (see key at top of table). Note that at the time of genotyping of line 6A, we used mice that were known to be heterozygous for *Tgfbm2 –129* (termed NIH line 6B), so that we could capture the diversity in both NIH.line 6 and NIH.*Tgfbm2–129* simultaneously. Hence, the 129 calls on chromosome 1 in line 6 mice originate from NIH.*Tgfbm2–129* rather than line 6.

Table S2. Summary of candidate gene amino acid polymorphisms between C57 and NIH compared to known amino acid residues in other mouse strains and species

Table S2

Table S3. Gamete competition output values for association to PAVM in Dutch HHT screen

Table S3

Table S4. Genetic association to PAVM in French HHT

Table S4